Unification of quantum Zeno–anti Zeno effects and parity-time symmetry breaking transitions

Jiaming Li ⓘ,* Tishuo Wang, and Le Luo ⓘ†

School of Physics and Astronomy, Sun Yat-Sen University, Zhuhai, Guangdong 519082, China

Sreya Vemuri and Yogesh N. Joglekar ⓘ

Department of Physics, Indiana University–Purdue University Indianapolis (IUPUI), Indianapolis, Indiana 46202, USA

The decay of an unstable quantum state can be inhibited or enhanced by tailored measurements, known as quantum Zeno effect (QZE) or anti Zeno effect (QAZE). QZE(QAZE) has been intensively explored in terms of the cases of various system-environment couplings, where the time evolution can be affected either by the projective measurements, or through the dissipative couplings to the environment. A general relation between QZE(QAZE) and the dissipation, for arbitrary dissipation strength and periodicity, is yet to be developed. In this paper, we show a framework to unify the QZE(QAZE) and the parity-time ($\mathcal{PT}$) symmetry breaking transition, where the pure dissipative Hamiltonian is mapped onto a $\mathcal{PT}$ symmetric non-Hermitian Hamiltonian. This method uses the $\mathcal{PT}$ symmetry transitions to distinguish QZE and QAZE, and can be applied to analyze the crossover behavior between these two effects. Using a heuristic example of a two-level system which is coupled to environment by periodical dissipation, we show the relation diagram between the QZE(QAZE) and the $\mathcal{PT}$ symmetry breaking transition, in which the QZE appears at an exceptional point that separates the $\mathcal{PT}$ symmetric (PTS) phase and the $\mathcal{PT}$ symmetry broken (PTSB) phase, and ends at the resonance point of the maximum $\mathcal{PT}$ symmetry breaking; after that, QAZE exists at the rest of the PTSB phase and remains in the next PTS phase. This interesting finding reveals a hidden relation between the QZE–QAZE and PTS-PTSB phases in a non-Hermitian quantum system.

I. INTRODUCTION

The quantum Zeno (anti Zeno) effect is an interesting feature of an open quantum system, initially interpreted as the fact that the evolution of the system can be suppressed (enhanced) by measuring it frequently enough in its initial state [1–10]. Over the years, these effects have been extensively used to control and manipulate quantum systems, including changing the decay rate of an unstable state [3,11–13], protecting quantum information [14], suppressing decoherence [8,15], extending the lifetime of ultracold molecules [16], and suppressing the tunneling in an optical lattice [11,17,18].

The implication of the term quantum Zeno effect–quantum anti Zeno effect [QZE(QAZE)] has since expanded, where the time evolution can be suppressed (enhanced) not only by projective measurements, but also by a variety of dissipative processes. Usually, a non-Hermitian term of dissipation $-i\gamma$ is inserted into the Hermitian Hamiltonian to play the role of the measurement [19,20]. Such non-Hermitian Hamiltonians are equivalent to those in a multimode Jaynes-Cummings model, enabling a unified theory to describe QZE (QAZE) for both repetitive and continuous observations.

However, it is still an open question whether there is a simple criterion to justify the deceleration (QZE) and acceleration (QAZE) of the evolution of a quantum system, not only in terms of projective measurements but also for the dissipation process. In Ref. [21], such criterion had been established for the case of frequently projective measurement, where the modified decay rate could be determined by the overlap between the reservoir's coupling spectrum and the spectrum of the state that is frequently measured. However, a general criterion, which could be extended to the dissipation with an arbitrary small strength, is still lacking. As explained in Ref. [21], such an extension is not trivial, because the effects of projective measurements can be treated as the phase randomization, and then induce level broadening consequently. But for small dissipations, we need to deal with partial decoherence which could induce the nontrival broadening of the quantum level described by a stochastic, nonlinear Liouville equation [22]. It is quite interesting to find out the relation between the QZE (QAZE) and the small dissipation with arbitrary strength and frequency, where the modified dynamics of the evolution usually do not behave as expected as the ideal projective measurements.

Recently, studies of passive $\mathcal{PT}$ symmetric quantum systems indicate the appearance of a slow decay mode associated with the $\mathcal{PT}$ symmetry broken (PTSB) phase [23–26]. Based on these findings, in this paper, we unify QZE (QAZE) and $\mathcal{PT}$ symmetry breaking transitions in terms of non-Hermitian

---

*lijiam29@mail.sysu.edu.cn
†luole5@mail.sysu.edu.cn

quantum mechanics. We find that $\mathcal{PT}$ symmetry breaking transitions play a general role in determining the appearance of QZE (QAZE). This treatment enables us to search for the QZE (QAZE) behaviors by analyzing the phase diagram of a $\mathcal{PT}$ symmetric non-Hermitian Hamiltonian. We show that the $\mathcal{PT}$ symmetry transitions hidden in a pure lossy two-level system could be used to precisely characterize QZE (QAZE) for dissipations with arbitrary strength and frequency.

II. GENERAL RELATIONS BETWEEN QZE (QAZE) AND PARITY-TIME SYMMETRY BREAKING TRANSITIONS

The relation between QZE (QAZE) and $\mathcal{PT}$ symmetry breaking transitions is described as follows: First, the projective measurement associated to QZE (QAZE) is considered as a strong dissipation that couples the system to environment. Then, by decreasing the dissipation strength, QZE (QAZE) is studied in the weak dissipation regime. This non-Hermitian Hamiltonian is given by

$$H = \nu_0|\uparrow\rangle\langle\uparrow| + (\nu - 2i\gamma)a^\dagger a + a^\dagger\Phi|\downarrow\rangle\langle\uparrow| + a\Phi^*|\uparrow\rangle\langle\downarrow|,$$
(1)

which describes a non-Hermitian system in which an atom in the excited state $|\uparrow\rangle$ of the energy ν_0 emits a single photon with frequency ν, and decays to the ground state $|\downarrow\rangle$ of zero energy. a ($a^\dagger$) is the annihilation (creation) operator for the photon mode, and Φ (Φ^*) is the coupling amplitude of the two atomic states. The action of the measurement is modeled by considering the photon mode is leakage with a dissipative rate γ [19].

Second, this dissipative Hamiltonian is mapped into a balanced gain-loss Hamiltonian with $\mathcal{PT}$ symmetry. Defining $\nu_a = (\nu_0 + \nu)/2$ and $\Delta = (\nu_0 - \nu)/2$, we have $H = H_0 + H_{\text{int}}$, where $H_0 = (-i\gamma + \nu_a)\mathbb{1} + \Delta\sigma_z$ with $\mathbb{1}$ is the unit matrix and σ_z the Pauli matrix, and we have

$$H_{\text{int}} = \begin{pmatrix} +i\gamma & \Phi^* \\ \Phi & -i\gamma \end{pmatrix}.$$
(2)

$H_{\text{int}} = \mathcal{PT}H_{\text{int}}\mathcal{PT}$ is a balanced gain-loss Hamiltonian which remains invariant under the $\mathcal{PT}$ operation. Here the parity operator is given by $\mathcal{P} = \sigma_x$ and the time-reversal operator is given by $\mathcal{T}i\mathcal{T} = -i$. This $\mathcal{PT}$ symmetric Hamiltonian allows symmetry breaking phase transitions in its eigenvalue spectrum, where the eigenvalues evolve from purely real numbers to complex-conjugate pairs. Known as passive $\mathcal{PT}$ symmetry transitions, the transitions of a no-gain system with mode-selective losses have been observed in various systems [23,24,26–39].

Third, the frequency-dependent analysis is applied to determine the QZE (QAZE) [40–43]. In the frequency-dependent picture, QZE(QAZE) is defined in a way that the effective decay rate Γ decreases (increases) as the measurement (dissipation) frequency ω increases. This definition provides a clear physical picture: the rapidly repeated measurements suppressed (enhanced) the relaxation process of the unstable state, leading to the QZE (QAZE).

For a static dissipation γ_0, it is well known that Γ increases as γ_0 increases in the $\mathcal{PT}$ symmetric (PTS) phase, but Γ decreases when increasing γ_0 in the PTSB phase. Here we
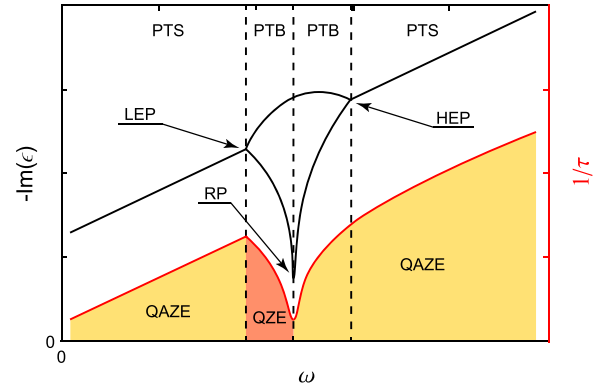

FIG. 1. The concept picture indicating the relation between QZE (QAZE) and $\mathcal{PT}$ symmetry breaking transitions. Black solid line: the dependence of the imaginary part of the quaienergy $-\text{Im}(\epsilon)$ of a passive $\mathcal{PT}$ symmetry Hamiltonian on ω. Red solid line: The effective lifetime τ of an unstable system. QZE (QAZE) represents quantum Zeno (anti Zeno) effect. PTS (PTSB) represents $\mathcal{PT}$ symmetric ($\mathcal{PT}$ symmetry broken) phase. LEP (HEP) is the exceptional point of $\mathcal{PT}$ symmetry breaking transitions with PTS at the low (high) frequency side. RP is the resonant point of the PTSB phase.

analyze how Γ depends on the magnitude and frequency of the time-periodically modulated dissipation $\gamma(t)$, where there exist rich phases separated by multiple PTS and PTSB phases [23,44]. In the PTS phase, Γ always increases as ω gets larger. While in the PTSB phase, the eigenvalues are split into two branches. One is called the "slow mode" with less imaginary (loss) components than the other "fast mode." The fast mode decays quickly, but the slow mode survives in the longer time and dominates the time evolution.

It is natural to ask whether a PTSB phase corresponds to the QZE while a PTS phase corresponds to the QAZE. The fact is that such simple one-to-one correspondence is invalid. Instead, we find a general relation, shown in Fig. 1, by analyzing the dependence of the imaginary part of the quasienergy $\text{Im}(\epsilon)$ on ω. In the PTS phase, $-\text{Im}(\epsilon)$ increases as ω becomes larger, resulting in the QAZE. When ω is larger than the lower exceptional point (LEP), the slow mode appears and the imaginary part of the slow mode decreases as ω increases. In the PTB regime, Γ is dominated by the slow mode that inhibits the decay, exhibiting the QZE until ω increases to the resonance point (RP). Above the RP, the imaginary part of the slow mode increases as ω increases, and the system shows the QAZE. The QAZE exists in the rest of the PTSB phase above the RP, and remains in the PTS phase above the higher exceptional point (HEP). This analysis uses the frequency response of a decay system to define the QZE (QAZE), only relying on the eigenmode behavior of a passive $\mathcal{PT}$ symmetric system. These arguments are rather general and do not depend on the details of the Hamiltonian, so we believe it could be a universal relation to unify parity-time symmetry breaking transitions and the QZE (QAZE) in open quantum systems.

III. MODEL AND RESULTS

To make the physics clear in a simple context, we illustrate the above relation using a two-level dissipative Rabi system driven by a resonant photon mode $H_L(t) = -J(t)(|\uparrow\rangle\langle\downarrow| +$

$|{\downarrow}\rangle\langle{\uparrow}|) - 2i\gamma(t)|{\downarrow}\rangle\langle{\downarrow}|$, in which the coupling rate $J(t)$ and the dissipation rate $\gamma(t)$ of the $|{\downarrow}\rangle$ level are both time dependent. As shown in Eq. (2), this Hamiltonian can be written as $H_L(t) = -i\gamma(t)\mathbb{1} + H_{PT}(t)$, where $H_{PT}(t) = -J(t)(|{\uparrow}\rangle\langle{\downarrow}| + |{\downarrow}\rangle\langle{\uparrow}|) + i\gamma(t)|{\uparrow}\rangle\langle{\uparrow}| - i\gamma(t)|{\downarrow}\rangle\langle{\downarrow}|$ is a $\mathcal{PT}$ symmetric Hamiltonian.

We assume a constant coupling rate J_0, and a square-wave modulation of the dissipation $\gamma(t)$ with the pulse width τ_1 and period T,

$$\gamma(t) = \begin{cases} \gamma_0, & 0 \leqslant t < \tau_1 \\ 0, & \tau_1 \leqslant t < T, \end{cases} \quad (3)$$

where $T = 2\pi/\omega$ is the period of the Hamiltonian, i.e., $H_L(t + T) = H_L(t)$. The PTS (PTSB) phase is defined via the quasienergies $\epsilon_F^{\pm}$ of the effective Floquet Hamiltonian, which are obtained from the nonunitary time evolution operator for one period $G'(T)$ (see Appendix A). Here $G'(T) = e^{-iH_L(t\geqslant\tau_1)(T-\tau_1)}e^{-iH_L(t<\tau_1)\tau_1} = e^{-\gamma_0\tau_1}G(T)$, with $G(T) = e^{-iH_{PT}(t\geqslant\tau_1)(T-\tau_1)}e^{-iH_{PT}(t<\tau_1)\tau_1}$ of the time evolution operator of balanced gain and loss. $\epsilon_F^{\pm}$ is then given by

$$\epsilon_F^{\pm} = -i\gamma_0\tau_1/T + i\ln(\Lambda_F^{\pm})/T \quad (4)$$

with $\Lambda_F^{\pm}$ of the eigenvalue of $G(T)$, and

$$\Lambda_F^{\pm} = c_1c_2 - \frac{J_0}{\epsilon_0}s_1s_2$$
$$\pm \sqrt{\left(\frac{\gamma_0}{\epsilon_0}s_1\right)^2 - \left(c_1s_2 + \frac{J_0}{\epsilon_0}s_1c_2\right)^2}. \quad (5)$$

The parameters are defined as $c_1 \equiv \cosh(\epsilon_0\tau_1)$, $c_2 \equiv \cos[J_0(T - \tau_1)]$, $s_1 \equiv \sinh(\epsilon_0\tau_1)$, $s_2 \equiv \sin[J_0(T - \tau_1)]$, and $\epsilon_0 \equiv \sqrt{\gamma_0^2 - J_0^2}$.

The imaginary parts of the quasienergies $\epsilon_F^{\pm}(\gamma_0, \omega, \tau_1)$ determine the decay rates $\Gamma_F^{\pm} = -2\,\mathrm{Im}\epsilon_F^{\pm}$. In the PTS phase, $\Lambda_F^{\pm}$ are complex conjugates and have the same magnitude. Therefore, the real parts of $\ln\Lambda_F^{\pm}$ are the same, and so are the imaginary parts of $\epsilon_F^{\pm}$. Thus $\Gamma_F^{\pm}$ are equal and increase when γ_0 increases. In the PTSB phase, both $\Lambda_F^{\pm}$ become purely real, leading to the imaginary parts of $\epsilon_F^{\pm}$ being different and the emergence of two different decay rates, named as slow mode and fast mode. Two modes arise at the exceptional point of the $\mathcal{PT}$ symmetry breaking transition. The degree of symmetry breaking is described by a dimensionless parameter $\mu(\gamma_0, \omega) = ||e^{-i\epsilon_F^+ T}| - |e^{-i\epsilon_F^- T}||$. As an example, Fig. 2(a) shows $\mu(\gamma_0, \omega)$ for the dissipation with the pulse parameter $J_0\tau_1 = 0.01$, and Fig. 2(b) shows Γ_F along the red-dashed line in Fig 2(a). The coincidence between the lifetime of the unstable state and the decay rates of the eigenmodes have been confirmed from large to small dissipation strength (Appendix C).

We could extend this result to the whole $\mathcal{PT}$ phase diagram as shown in Fig. 2. There are multiple PTS and PTSB blocks with the resonant frequencies of PTSB $\omega_n/J_0 = 2/n$, where $n = 1, 2, 3 \ldots$ (see Appendix B). In one of the PTS blocks (marked as ①) shown in Fig. 2, $\Gamma_F^{\pm}$ decreases with the decrease of ω, which indicates QAZE. As ω decreases, the system experiences a phase transitions from PTS to PTSB. After crossing the exceptional point, in one of the PTSB
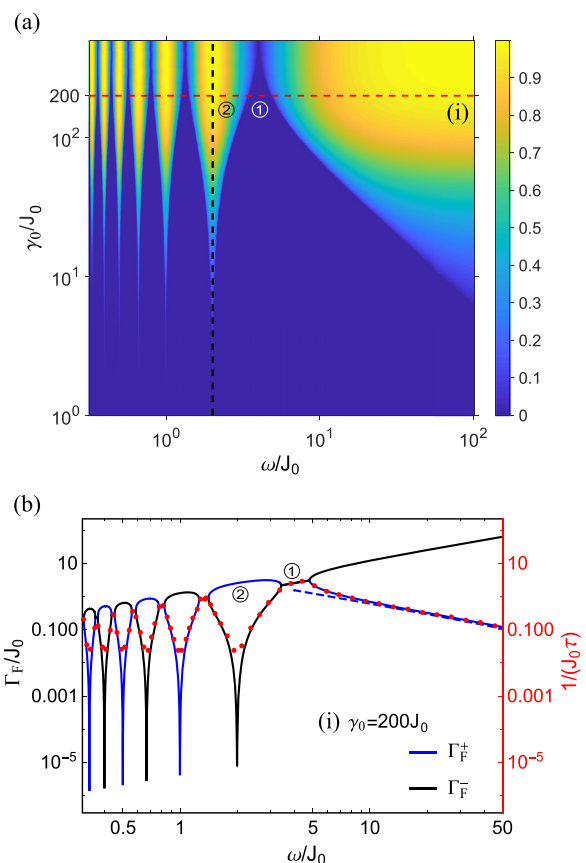

FIG. 2. The decay rates of a two-level system with a time-dependent dissipation modeled by a $\mathcal{PT}$ symmetric Hamiltonian. (a) The phase diagram of $\mathcal{PT}$ symmetry breaking, in which the color presents $\mu(\gamma_0, \omega)$. The vertical axis is the normalized dissipation amplitude γ_0/J_0, and the horizontal axis is normalized modulation frequency ω/J_0. Note that the phase diagram is obtained by fixing $\tau_1 = 0.01/J_0$ and varying T. Although the widths of the PTS phases (deep-blue color) and the PTSB phases (all other colors) depend on τ_1, the structure of the phase diagram as well as the location of the resonance peaks (one of them represented by the black-dashed line) does not depend on τ_1. (b) The comparison of the decay rates Γ_F and the lifetime τ along the red-dashed line in Fig. 2(a) with $\gamma_0 = 200J_0$. The red dot is the numerical simulation of the lifetime of the unstable state. ① (②) presents one of the PTS (PTSB) regimes.

blocks (marked as ②), the decay rate of the slow mode is not monotonous. Below the PTSB resonance, Γ_F^- decreases with the increase of ω, but has the reverse behavior above the resonance. So the transition from the QAZE to the QZE is at the point of ω_n.

IV. DISCUSSION AND CONCLUSIONS

This framework leads to the unification of the $\mathcal{PT}$ symmetry breaking transition and the QZE (QAZE). But is this picture also supported by the results of the case of the projective measurements and the case of continuous observation (static dissipation)? The answer is yes. In the following, we confirm the universality of this unification for both cases.

First, we discuss the projective measurements by considering the limit of the large and frequent dissipation
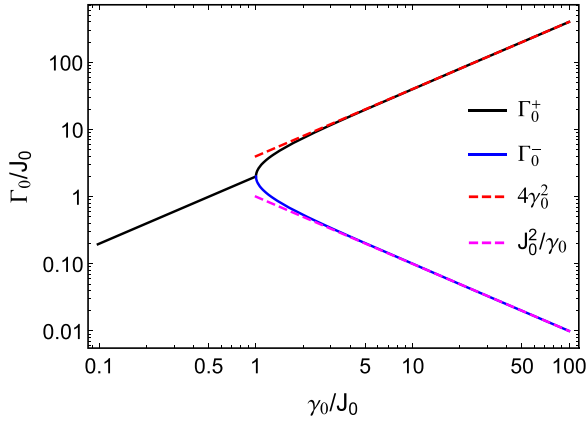
FIG. 3. The decay rates of continuous observation as a function of the static dissipation. The black (blue) line represents the eigenmode Γ_0^+ (Γ_0^-) in the PTSB phase, respectively (the two eigenmodes overlap in the PTS phase). The dashed lines represent the decay rates at the limit of $\gamma_0 \gg J_0$.

with $\gamma_0/J_0 \gg 1$ and $\omega/J_0 \gg 1$. The decay rate of the states $\Gamma_F^{\pm}$ is simplified as $\Gamma_F^{\pm} = (J_0^2/\gamma_0)(\tau_1/T) + 2 \ln[c_2 \pm \sqrt{1-s_2^2}/2]/T$. With $\omega/J_0 \gg 1$, $\cos(J_0\tau_2) \to e^{-(J_0\tau_2)^2/2}$, we got

$$\Gamma_F^+ = \frac{J_0^2}{\gamma_0}\frac{\tau_1}{T} + J_0^2\frac{\tau_2^2}{T}. \tag{6}$$

On the other hand, the QZE appears in a two-level system in which the projective measurements are applied to the final state [8]. In this system, the two-level system is driven with the Rabi frequency ω_R and the initial population is in the $|\uparrow\rangle$ level, while the final state $|\downarrow\rangle$ couples to the third state with a dissipative rate γ_c. When the N rapid projective measurements with the time intervals of $\delta t = t/N$ are applied to the final state, the survival probability of the initial state after N times measurements is $p^N(t) = p(\delta t)^N \simeq [1 - (\omega_R\delta t/2)^2]^N$. When $\delta t \ll \pi/\omega_R$, the decay rate of $p^N(t)$ is $1/\tau_{QZE} = \omega_R^2\delta t/4$, showing that the projective measurements slow down the decay of the state. In the real experiments, the measurement time is finite, and both the measurement pulse duration t_p and the time interval between the two consecutive pulses δt are required to be calculated, giving the decay rate (see Appendix A)

$$\frac{1}{\tau} = \frac{\omega_R^2}{\gamma_c}\frac{t_p}{t_p + \delta t} + \frac{\omega_R^2}{4}\frac{\delta t^2}{t_p + \delta t}. \tag{7}$$

It is obvious that Eqs. (6) and (7) are equivalent, which indicates that QZE (QAZE) can be well understood in terms of the picture of $\mathcal{PT}$ symmetry breaking transition. The blue-dashed line in Fig. 2(b) is plotted in Eq. (7), showing that the two decay rates are in good agreement with each other.

Second, we consider the continuous observation (static dissipation). In the static case, the eigenvalues are given by $\lambda_{\pm} = -i\gamma_0 \pm \sqrt{J_0^2 - \gamma_0^2}$ where J_0, γ_0 are the static parameters. The decay rates $\Gamma_0^{\pm}$ as a function of γ_0/J_0 are shown in Fig. 3. When $\gamma_0 \leqslant J_0$ with the J_0 as the LEP, the system is in the PTS phase and the decay rates of the two eigenmodes are equal, $\Gamma_0^{\pm} = 2\gamma_0$. In this phase, the decay rate increases as

γ_0 increases. When $\gamma_0 > J_0$, the system is in the PTSB phase, leading to the emergence of two modes given by

$$\Gamma_0^- = 2\left(\gamma_0 - \sqrt{\gamma_0^2 - J_0^2}\right) \underset{\gamma_0 \gg J_0}{\to} \frac{J_0^2}{\gamma_0},$$

$$\Gamma_0^+ = 2\left(\gamma_0 + \sqrt{\gamma_0^2 - J_0^2}\right) \underset{\gamma_0 \gg J_0}{\to} 4\gamma_0. \tag{8}$$

In the limit $\gamma_0 \gg J_0$, the decay rate for the fast mode doubles, $\Gamma_0^+ \to 4\gamma_0$, whereas that for the slow mode vanishes, $\Gamma_0^- \to J_0^2/\gamma_0$. These values coincide with the continuous QZE case with the theory in Ref. [19] and experiment in Ref. [8]. The populations of up and down level decays are given by $1/\tau_{|\uparrow\rangle} = \omega_R^2/\gamma_c$ and $1/\tau_{|\downarrow\rangle} = \gamma_c$ from the picture of quantum measurement. It is clear that the two approaches are equivalent provided $\omega_R = 2J_0$ and $\gamma_c = 4\gamma_0$. In the strong-dissipation limit $\gamma_0 \gg J_0$, the slowly decaying eigenmode has a near-unity overlap with the $|\uparrow\rangle$, while the rapidly decaying eigenmode is mostly aligned with $|\downarrow\rangle$. Thus, the PTSB phase provides a suitable generalization of the continuous QZE when the dissipation strength is moderate, $\gamma_0 \gtrsim J_0$. On the other hand, when $\gamma_0 \leqslant J_0$, the two decay rates $\Gamma_0^{\pm} = 2\gamma_0$ increase with increasing dissipation, which is consistent with the QAZE.

We formulate a general picture of QZE(QAZE) in the two-level dissipative Rabi system based on the phase diagram of $\mathcal{PT}$ symmetry. QZE is always observed in the strong dissipative regime $\gamma_0/J_0 \gg 1$ above a certain modulation frequency ω. But, even deep in the strong-dissipation regime, the QAZE could also exist in the regime near the EP points. On the other hand, in the weak-dissipation regime, the QAZE is observed at most of the modulation frequencies. Conversely, although the QZE survives down to vanishingly small dissipation strengths, i.e., $\gamma_0/J_0 \ll 1$, it only exists with the modulation frequencies in the range between the LEP and the RP of the PTSB phase.

In conclusion, we unify the symmetry transitions associated to the $\mathcal{PT}$ symmetric non-Hermitian Hamiltonians with the quantum measurement effect of QZE (QAZE). Using a dissipation term, instead of projective measurement, the interaction between the unstable system and the environment can be tuned from strong to weak, enabling a systematic study of tunable dissipation, in which QZE(QAZE) is not as manifested as in the projective measurement case. We find that $\mathcal{PT}$ symmetry breaking transitions exist with the appearance of the QZE(QAZE), regardless of strong or weak dissipations [45], or periodical or static ones. A recent experimental work with a momentum lattice of cold atoms has partially confirmed our predictions [46]. Our findings help to explore QZE(QAZE) physics in complex setups, such as systems beyond Markovian approximation [40,47] and with many-body interactions [48,49]. With a simple and quantitative criterion, our method could lead to a deep understanding of the relations between the quantum measurement effects and the non-Hermitian quantum dynamics.

The data that support the findings of this study are available from the corresponding author upon reasonable request.

APPENDIX A: THE DECAY RATE OF A DISSIPATIVE TWO-LEVEL SYSTEM WITH A $\mathcal{PT}$ SYMMETRIC HAMILTONIAN

The PTS (PTSB) phases of the passive $\mathcal{PT}$ symmetric Hamiltonian H_L are defined via quasienergies $\epsilon_F^{\pm}$, which are obtained from the eigenvalues of the nonunitary time evolution operator of one period $G'(T)$ [23–26]:

$$G'(T) = e^{-\gamma_0\tau_1}G(T). \tag{A1}$$

The quasienergies $\epsilon_F^{\pm}$ of $G'(T)$ are related to the time evolution operator $G(T)$ of a balanced gain-loss Hamiltonian $H_{\mathcal{PT}}$, given by

$$\epsilon_F^{\pm} = -i\gamma_0\tau_1/T + (i/T)\ln(\Lambda_F^{\pm}), \tag{A2}$$

where $\Lambda_F^{\pm}$ are eigenvalues of $G(T)$.

The time evolution operator for one period of the $\mathcal{PT}$ system with the square-wave dissipative term is given by

$$G(T) = G_u(\tau_2)G_{\mathcal{PT}}(\tau_1) = e^{iJ\sigma_x\tau_2}e^{-iH_{\mathcal{PT}}\tau_1} = \begin{pmatrix} c_2 & is_2 \\ is_2 & c_2 \end{pmatrix}\begin{pmatrix} c_1 + \frac{\gamma_0}{\epsilon_0}s_1 & \frac{iJ_0}{\epsilon_0}s_1 \\ \frac{iJ_0}{\epsilon_0}s_1 & c_1 - \frac{\gamma_0}{\epsilon_0}s_1 \end{pmatrix}$$

$$= \begin{pmatrix} (c_1c_2 - \frac{J_0}{\epsilon_0}s_1s_2) + \frac{\gamma_0}{\epsilon_0}s_1c_2 & i(c_1s_2 + \frac{J_0}{\epsilon_0}s_1c_2) - i\frac{\gamma_0}{\epsilon_0}s_1s_2 \\ i(c_1s_2 + \frac{J_0}{\epsilon_0}s_1c_2) + i\frac{\gamma_0}{\epsilon_0}s_1s_2 & (c_1c_2 - \frac{J_0}{\epsilon_0}s_1s_2) - \frac{\gamma_0}{\epsilon_0}s_1c_2 \end{pmatrix}$$

$$= \left(c_1c_2 - \frac{J_0}{\epsilon_0}s_1s_2\right)\mathbb{1} + \frac{\gamma_0}{\epsilon_0}s_1c_2\sigma_z + \frac{\gamma_0}{\epsilon_0}s_1s_2\sigma_y + i\left(c_1s_2 + \frac{J_0}{\epsilon_0}s_1c_2\right)\sigma_x. \tag{A3}$$

Here, $\tau_2 \equiv T - \tau_1$, and the eigenvalues of $G(T)$ are

$$\Lambda_F^{\pm} = c_1c_2 - \frac{J_0}{\epsilon_0}s_1s_2 \pm \sqrt{\left(\frac{\gamma_0}{\epsilon_0}s_1\right)^2 - \left(c_1s_2 + \frac{J_0}{\epsilon_0}s_1c_2\right)^2}, \tag{A4}$$

where $c_1 \equiv \cosh(\epsilon_0\tau_1)$, $c_2 \equiv \cos(J_0\tau_2)$, $s_1 \equiv \sinh(\epsilon_0\tau_1)$, $s_2 \equiv \sin(J_0\tau_2)$, and $\epsilon_0 \equiv \sqrt{\gamma_0^2 - J_0^2}$. $\Lambda_F^{\pm}$ are rewritten as

$$\Lambda_F^{\pm} = \frac{1}{2}e^{\epsilon_0\tau_1}\left\{(1 + e^{-2\epsilon_0\tau_1})c_2 - \frac{J_0}{\epsilon_0}(1 - e^{-2\epsilon_0\tau_1})s_2 \pm \sqrt{\left[\frac{\gamma_0}{\epsilon_0}(1 - e^{-2\epsilon_0\tau_1})\right]^2 - \left[(1 + e^{-2\epsilon_0\tau_1})s_2 + \frac{J_0}{\epsilon_0}(1 - e^{-2\epsilon_0\tau_1})c_2\right]^2}\right\}. \tag{A5}$$

In the limit of strong dissipation $J_0/\gamma_0 \to 0$, we have

$$\epsilon_0 = \gamma_0\sqrt{1 - \left(\frac{J_0}{\gamma_0}\right)^2} \to \gamma_0 - \frac{J_0^2}{2\gamma_0},$$

$$\frac{J_0}{\epsilon_0} = \frac{J_0}{\gamma_0\sqrt{1 - \left(\frac{J_0}{\gamma_0}\right)^2}} \to 0,$$

$$\frac{\gamma_0}{\epsilon_0} = \frac{1}{\sqrt{1 - \left(\frac{J_0}{\gamma_0}\right)^2}} \to 1,$$

$$e^{-2\epsilon_0\tau_1} = e^{-2(\gamma_0/J_0)\sqrt{1-(J_0/\gamma_0)^2}J_0\tau_1} \to 0. \tag{A6}$$

Therefore, $\Lambda_F^{\pm}$ can be simplified into

$$\Lambda_F^{\pm} = \frac{1}{2}e^{[\gamma_0 - (J_0^2/2\gamma_0)]\tau_1}\left(c_2 \pm \sqrt{1 - s_2^2}\right). \tag{A7}$$

Then the decay rates of the states $\Gamma_F^{\pm}$ become

$$\Gamma_F^{\pm} = \frac{J_0^2}{\gamma_0}\frac{\tau_1}{T} - \frac{2}{T}\ln\left[\frac{1}{2}\left(c_2 \pm \sqrt{1 - s_2^2}\right)\right]. \tag{A8}$$

If the system is in the strong-dissipation limit as well as in the high-frequency limit $\omega/J_0 \gg 1$, $J_0\tau_2 \to 0$, $c_2 \to 1 - (J_0\tau_2)^2/2 \to e^{-(J_0\tau_2)^2/2}$. Then Γ_F^+ is further simplified as

$$\Gamma_F^+ = \frac{J_0^2}{\gamma_0}\frac{\tau_1}{T} + J_0^2\frac{\tau_2^2}{T}. \tag{A9}$$

This result coincides with the formula obtained from the formula of QZE induced by the projective frequent measurement [8].

Here, we present the details about the derivation of Eq. (7) (in the main text). We define Γ_p as the decay rate for the pulse duration t_p, which is ω_R^2/γ_c. Here, $\gamma_c/2 = 2\gamma_0$ equals the decay rate of the $|\downarrow\rangle$. We also define Γ_c as the decay rate for the separation duration δt of the pulses, which is $\omega_R^2\delta t/4$. Thus, the survival probability of the stable system after N measurement cycles is

$$P(t) = (e^{-\Gamma_p t_p}e^{-\Gamma_c\delta t})^N = e^{-\Gamma_p Nt_p}e^{-\Gamma_c N\delta t} = e^{-\Gamma_e N(t_p+\delta t)}, \tag{A10}$$

where Γ_e is the equivalent lifetime. So,

$$-\Gamma_c N\delta t - \Gamma_p Nt_p = -\Gamma_e N(t_p + \delta t),$$

$$\Gamma_e = \Gamma_p\frac{t_p}{t_p + \delta t} + \Gamma_c\frac{\delta t}{t_p + \delta t},$$
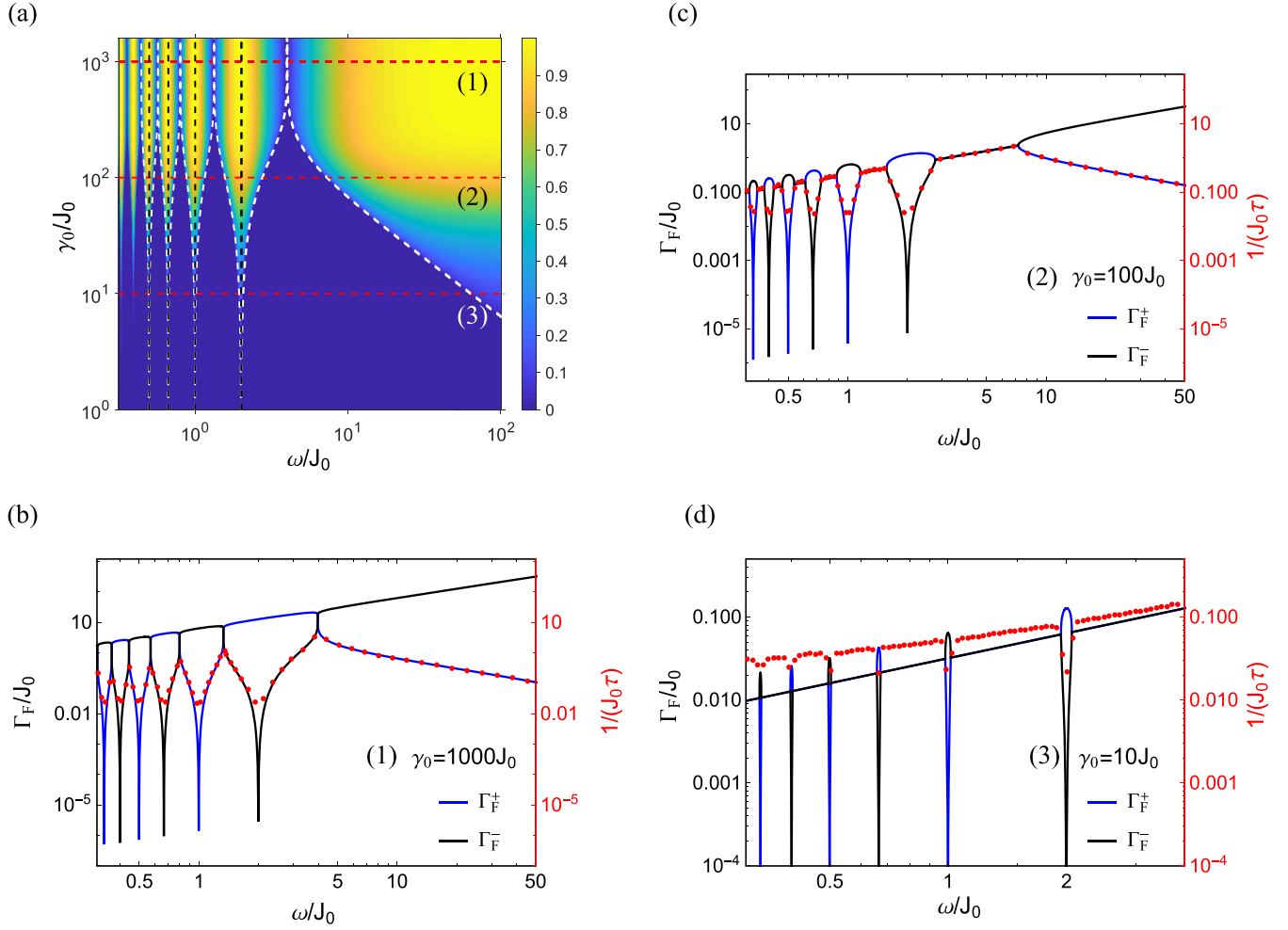
FIG. 4. The decay rates of a two-level system with different dissipation strengths. Axis and labels are the same as Fig. 2 in the main paper. (a) The phase diagram of $\mathcal{PT}$ symmetry breaking. White-dash lines present the LEPs and HEPs. Black-dash lines are the RPs of the PTB phases. (b), (c), (d) The comparison of the decay rates Γ_F of the eigenmodes and the lifetime of the unstable state, along the red-dashed lines in (a) with $\gamma_0=1000J_0$, $100J_0$, and $10J_0$, respectively.

$$1/\tau = \Gamma_e = \frac{\omega_R^2}{\gamma_c}\frac{t_p}{t_p+\delta t} + \frac{\omega_R^2}{4}\frac{\delta t^2}{t_p+\delta t}. \quad (A11)$$

Note that the same equation can be also found in Eq. (5) of Ref. [8].

APPENDIX B: THE PARAMETERS OF THE PTS AND PTSB PHASES

The exceptional lines. The PTS (PTSB) phases are determined by the properties of $\Lambda_F^{\pm}$ [23,44], given by

$$P(y) = \left[\frac{\gamma_0}{\epsilon_0}(1-e^{-2\epsilon_0\tau_1})\right]^2$$
$$- \left[(1+e^{-2\epsilon_0\tau_1})\sin y + \frac{J_0}{\epsilon_0}(1-e^{-2\epsilon_0\tau_1})\cos y\right]^2, \quad (B1)$$

where $y = J_0\tau_2 = J_0(2\pi/\omega - \tau_1)$. When $P(y)=0$, the LEP ω_{Ln} and the HEP ω_{Hn} are solved as

$$\frac{\omega_{Hn}}{J_0} = \frac{2\pi}{\arccos\left(-\frac{J_0}{\gamma_0}-\frac{\epsilon_0^2}{J_0\gamma_0+\gamma_0^2 c_1}\right) + J_0\tau_1 + n\pi},$$

$$\frac{\omega_{Ln}}{J_0} = \frac{2\pi}{\arccos\left(\frac{J_0}{\gamma_0}+\frac{\epsilon_0^2}{J_0\gamma_0+\gamma_0^2 c_1}\right) + J_0\tau_1 + n\pi}, \quad (B2)$$

where $n = 0, 1, 2\ldots$ is the transition index from higher to lower frequency. Note that the index n of the two exceptional lines of a PTSB phase are different by one.

The resonant point of PTSB. In the weak-dissipation limit of $\gamma_0/J_0 \to 0$, there are some PTSB regimes.

$$\epsilon_0 = J_0\sqrt{\left(\frac{\gamma_0}{J_0}\right)^2 - 1} \to iJ,$$

$$\frac{J_0}{\epsilon_0} = \frac{1}{\sqrt{\left(\frac{\gamma_0}{J_0}\right)^2 - 1}} \to -i,$$

$$\frac{\gamma_0}{\epsilon_0} = \frac{\gamma_0}{J_0\sqrt{\left(\frac{\gamma_0}{J_0}\right)^2 - 1}} \to 0,$$

$$c_1 = \cos\left(\sqrt{J_0^2 - \gamma_0^2}\,\tau_1\right) \to \cos(J_0\tau_1),$$

$$s_1 = i\sin\left(\sqrt{J_0^2 - \gamma_0^2}\,\tau_1\right) \to i\sin(J_0\tau_1). \qquad (B3)$$

$\Lambda_F^{\pm}$ are simplified into

$$\Lambda_F^{\pm} = \cos(J_0 T) \pm i\sqrt{\sin^2(J_0 T)}. \qquad (B4)$$

Only when $J_0 T = n\pi$, $n = 1, 2, 3\ldots$, $\Lambda_F^{\pm}$ are purely real, indicating the resonant points

$$\frac{\omega_n}{J_0} = \frac{2}{n}, \quad n = 1, 2, 3\ldots. \qquad (B5)$$

The resonant points of the PTSB are shown by the dark-dashed lines in Fig. 4(a).

APPENDIX C: THE DECAY RATES OF THE UNSTABLE STATES

Based on the unified picture of QZE(QAZE) and $\mathcal{PT}$ symmetry transition, the lifetime of the unstable state and the decay rates of the eigenmodes should coincide. We confirm this by numerically calculating the population number occupied in the unstable state and then fitting the lifetime, and use this result to compare the calculation of eigenmodes shown in Figs. 4(b)–4(d).

[1] B. Misra and E. C. G. Sudarshan, The Zeno's paradox in quantum theory, J. Math. Phys. **18**, 756 (1977).

[2] W. C. Schieve, L. P. Horwitz, and J. Levitan, Numerical study of zeno and anti-zeno effects in a local potential model Phys. Lett. A, **136**, 264 (1989).

[3] W. M. Itano, D. J. Heinzen, J. J. Bollinger, and D. J. Wineland, Quantum Zeno effect Phys. Rev. A, **41**, 2295 (1990).

[4] D. Home and M. A. B. Whitaker, A conceptual analysis of quantum Zeno; paradox, measurement, and experiment Ann. Phys., **258**, 237 (1997).

[5] P. Facchi, V. Gorini, G. Marmo, S. Pascazio, and E. C. G. Sudarshan, Quantum Zeno dynamics Phys. Lett. A, **275**, 12-19 (2000).

[6] M. Lewenstein and K. Rzazewski, Quantum anti-Zeno effect Phys. Rev. A, **61**, 022105 (2000).

[7] B. Kaulakys and V. Gontis, Quantum anti-Zeno effect Phys. Rev. A, **56**, 1131 (1997).

[8] E. W. Streed, J. Mun, M. Boyd, G. K. Campbell, P. Medley, W. Ketterle, and D. E. Pritchard, Continuous and Pulsed Quantum Zeno Effect Phys. Rev. Lett., **97**, 260402 (2006).

[9] P. Facchi, H. Nakazato, and S. Pascazio, From the Quantum Zeno to the Inverse Quantum Zeno Effect Phys. Rev. Lett., **86**, 2699 (2001).

[10] P. Facchi and M. Ligabo, Quantum Zeno effect and dynamics J. Math. Phys., **51**, 022103 (2010).

[11] M. C. Fischer, B. Gutiérrez-Medina, and M. G. Raizen, Observation of the Quantum Zeno and Anti-Zeno Effects in an Unstable System Phys. Rev. Lett. **87**, 040402 (2001).

[12] B. Yan, S. A. Moses, B. Gadway, J. P. Covey, K. R. A. Hazzard, A. M. Rey, D. S. Jin, and J. Ye, Observation of dipolar spin-exchange interactions with lattice-confined polar molecules Nature **501**, 521 (2013).

[13] M. Zhang, W. Wu, L. He, Y. Xie, C. Wu, Q. Li, and P. Chen, Demonstration of quantum anti-Zeno effect with a single trapped ion Chin. Phys. B, **27**, 090305 (2018).

[14] S. Hacohen-Gourgy, L. P. Garcia-Pintos, L. S. Martin, J. Dressel, and I. Siddiqi, Incoherent Qubit Control Using the Quantum Zeno Effect Phys. Rev. Lett., **120**, 020505 (2018).

[15] J. M. Raimond, P. Facchi, B. Peaudecerf, C. Pascazio, C. Sayrin, I. Dotsenko, S. Gleyzes, M. Brune, and S. Haroche, Quantum Zeno dynamics of a field in a cavity, Phys. Rev. A **86**, 032120 (2012).

[16] B. Zhu, B. Gadway, M. Foss-Feig, J. Schachenmayer, M. L. Wall, R. A. Hazzard, B. Yan, S. A. Moses, J. P. Covey, D. S. Jin et al., Suppressing the Loss of Ultracold Molecules Via the Continuous Quantum Zeno Effect, Phys. Rev. Lett. **112**, 070404 (2014).

[17] Y. S. Patil, S. Chakram, and M. Vengalattore, Measurement-Induced Localization of an Ultracold Lattice Gas, Phys. Rev. Lett. **115**, 140402 (2015).

[18] Y. J. Han, Y. H. Chan, W. Yi, A. J. Daley, S. Diehl, P. Zoller, and L. M. Duan, Stablization of p-Wave Superfluid State in an Optical Lattice, Phys. Rev. Lett. **103**, 070404 (2009).

[19] L. S. Schulman, Continuous and pulsed observations in the quantum Zeno effect, Phys. Rev. A **57**, 1509 (1998).

[20] J. G. Muga, J. Echanobe, A. Campo, and I. Lizuain, Generalized relation between pulsed and continuous measurements in the quantum Zeno effect, J. Phys. B: At., Mol. Opt. Phys. **41**, 175501 (2008).

[21] A. G. Kofmann and G. Kurizki, Acceleration of quantum decay processes by frequent observations, Nature (London) **405**, 546 (2000).

[22] M. Grigorescu, Decoherence and dissipation in quantum two-state systems, Phys. A (Amsterdam, Neth.) **256**, 149 (1998).

[23] J. Li, A. K. Harter, J. Liu, L. de Melo, Y. N. Joglekar, and L. Luo, Observation of parity-time symmetry breaking transitions in a dissipative Floquet system of ultracold atoms, Nat. Commun. **10**, 855 (2019).

[24] M. Naghiloo, M. Abbasi, Y. N. Joglekar, and K. M. Murch, Quantum state tomography across the exceptional point in a single dissipative qubit, Nat. Phys. **15**, 1232 (2019).

[25] Y. N. Joglekar and A. K. Harter, Passive parity-time-symmetry-breaking transitions without exceptional points in dissipative photonic systems, Photonics Res. **6**, A51 (2018).

[26] R. J. León-Montiel, M. A. Quiroz-Juárez, J. L. Domínguez-Juárez, R. Quintero-Torres, J. L. Aragón, A. K. Harter, and Y. N. Joglekar, Observation of slowly decaying eigenmodes without exceptional points in Floquet dissipative synthetic circuits, Commun. Phys. **1**, 88 (2018).

[27] A. Guo, G. J. Salamo, D. Duchesne, R. Morandotti, M. Voltatier-Ravat, V. Aimez, G. A. Siviloglou, and D. N. Christodoulides, Observation of $\mathcal{PT}$-Symmetry Breaking in Complex Optical Potentials, Phys. Rev. Lett. **103**, 093902 (2009).

[28] C. E. Ruter, K. G. Makris, R. El-Ganainy, D. N. Christodoulides, M. Segev, and D. Kip, Observation of parity-time symmetry in optics, Nat. Phys. **6**, 192 (2010).

[29] A. Regensburger, C. Bersch, M. Miri, G. Onishchukov, D. N. Christodoulides, and U. Peschel, Parity-time synthetic photonic lattices, Nature (London) **488**, 167 (2012).

[30] W. D. Heiss, The physics of exceptional points, J. Phys. A: Math. Theor. **45**, 444016 (2012).

[31] M. Chitsazi, H. Li, F. M. Ellis, and T. Kottos, Experimental Realization of Floquet $\mathcal{PT}$-Symmetric Systems, Phys. Rev. Lett. **119**, 093901 (2017).

[32] J. Schindler, A. Li, M. C. Zheng, F. M. Ellis, and T. Kottos, Experimental study of active LRC circuits with $\mathcal{PT}$ symmetries, Phys. Rev. A **84**, 040101(R) (2011).

[33] S. Assawaworrarit, X. Yu, and S. Fan, Robust wireless power transfer using a nonlinear parity-time-symmetric circuit, Nature (London) **546**, 387 (2017).

[34] B. Peng, S. K. Ozedemir, F. Lei, F. Monifi, M. Gianfreda, G. L. Long, S. Fan, F. Nori, C. M. Bender, and L. Yang, Parity-time-symmetric whispering-gallery microcavities, Nat. Phys. **10**, 394 (2013).

[35] H. Xu, D. Mason, L. Jiang, and J. G. E. Harris, Topological energy transfer in an optomechanical system with exceptional points, Nature (London) **537**, 80 (2016).

[36] J. Xu, Y. X. Du, W. Huang, and D. W. Zhang, Detecting topological exceptional points in a parity-time sysmmetric system with cold atoms, Opt. Express **25**, 15786 (2017).

[37] L. Xiao, X. Zhan, Z. H. Bian, K. K. Wang, X. Zhang, X. P. Wang, J. Li, D. Kim, N. Kawakami, W. Yi, H. Obuse, B. C. Sanders, and P. Xue, Observation of topological edge states in parity-time-symmetric quantum walks, Nat. Phys. **13**, 1117 (2017).

[38] M. Brandstetter, M. Liertzer, C. Deutsch, P. Klang, H. Schoberl, H. E. Tureci, G. Strasser, K. Unterrainer, and S. Rotter, Reversing the pump dependence of a laser at an exceptional point, Nat. Commun. **5**, 4034 (2014).

[39] Y. Wu, W. Liu, J. Geng, X. Song, X. Ye, C.-K. Duan, X. Rong, and J. Du, Observation of parity-time symmetry breaking in a single-spin system, Science **364**, 878 (2019).

[40] W. Wu and H. Q. Lin, Quantum Zeno and anti-Zeno effects in quantum dissipative systems, Phys. Rev. A **95**, 042132 (2017).

[41] Y. R. Zhang and H. Fan, Zeno dynamics in quantum open systems, Sci. Rep. **5**, 11509 (2015).

[42] A. Z. Chaudhry, A general framework for the Quantum Zeno and anti-Zeno effects, Sci. Rep. **6**, 29497 (2016).

[43] A. Z. Chaudhry and J. B. Gong, Zeno and anti-Zeno effects on dephasing, Phys. Rev. A **90**, 012101 (2014).

[44] Y. N. Joglekar, R. Marathe, P. Durganandini, and R. K. Pathak, $\mathcal{PT}$ spectroscopy of the Rabi problem, Phys. Rev. A **90**, 040101(R) (2014).

[45] K. Snizhko, P. Kumar, and A. Romito, Quantum Zeno effect appears in stages, Phys. Rev. Res. **2**, 033512 (2020).

[46] T. Chen, W. Gou, D. Xie, T. Xiao, W. Yi, J. Jing, and B. Yan, Quantum Zeno effects across a parity-time symmetry breaking transition in atomic momentum space, npj Quantum Inf. **7**, 78 (2021).

[47] Z. Zhou, Z. Lü, H. Zheng, and H. S. Goan, Quantum Zeno and anti-Zeno effects in open quantum systems, Phys. Rev. A **96**, 032101 (2017).

[48] Y. Li, X. Chen, and M. P. A. Fisher, Quantum Zeno effect and the many-body entanglement transition, Phys. Rev. B **98**, 205136 (2018).

[49] F. Heinrich, M. Christopher, K. Corinna, C. Alessio, and D. Sebastian, Ultracold quantum wires with localized losses: many-body quantum Zeno effect, Phys. Rev. B **101**, 144301 (2020).